ELSEVIER

International Journal of Heat and Fluid Flow 22 (2001) 343–349

International Journal of HEAT AND FLUID FLOW

www.elsevier.com/locate/ijhff

Comparison of state-of-the-art droplet turbulence interaction models for jet engine combustor conditions

G. Klose *, B. Rembold, R. Koch, S. Wittig

Institut für Thermische Strömungsmaschinen, Universität Karlsruhe (TH), Kaiserstr. 12, 76128 Karlsruhe, Germany

Abstract

The objective of this paper is to assess three state-of-the-art Lagrangian droplet turbulence interaction models for jet engine combustor operating conditions. The models can be distinguished by their underlying temporal autocorrelation function of the gaseous velocity fluctuations seen by a droplet. Two generic experiments and one realistic test case were used for validation of the models. The analysis of single particle dispersion revealed poor accuracy of the model proposed by Gosman and Ioannides at small Stokes numbers and high relative velocities. The models of Milojević and of Blümcke gave good agreement with the experimental data. Furthermore, the accuracy of the three models in predicting real polydisperse combustor sprays was studied. It is concluded that the droplet turbulence model does not affect significantly the overall combustor prediction. Finally, characteristic parameters describing monodisperse particle dispersion have been extracted by a numerical study based on the model of Blümcke covering a wide range of combustor operation conditions. These parameters are compared to analytical results of Wang et al.

1. Introduction

A key aspect for correctly predicting jet engine combustion are the models representing the mixing of the evaporating fuel spray with air. To capture the effect of turbulent particle dispersion, different models have been developed in the past (Gosman and Ioannides, 1983; Milojević, 1990; Berlemont et al., 1990; Blümcke, 1992; Dutta et al., 1997). However, only little information about the exactness of these models for predicting combustor sprays is available from the literature (Chen and Pereira, 1994; Klose et al., 2000).

The purpose of this paper is to assess three state-of-the-art Lagrangian particle turbulence models for predicting droplet dispersion under combustor operating conditions. The eddy lifetime models of Gosman and Ioannides (1983) and Milojević (1990) as well as the spectral dispersion model suggested by Blümcke (1992) are compared for two test cases. In the first test case, the predictions of monodisperse particle dispersion are fundamentally assessed by means of generic experimental data provided by Snyder and Lumley (1971). This test case was also used by Gosman and Ioannides, Milojević and Blümcke to validate their models. However, in the framework of this study, a comparison of the three models is presented which can be used as a basis to select the appropriate model. In a subsequent step, the study is extended to the case of a polydisperse real fuel spray which was experimentally investigated at the Institute for Thermal Turbomachinery (Willmann, 1999).

Finally, a parametric study elaborating characteristic parameters of the dispersion process is presented. It covers, in contradiction to the experimental test case, a wide range of possible dispersion conditions which are typical for aero-engine combustors. The results are based on the spectral dispersion model of Blümcke which was found to be in good agreement with the experimental data, as shown in the first part of the paper.

2. Review of Lagrangian droplet turbulence models

The prediction of droplet propagation within the Lagrangian frame of reference is based on the solution of the equations of droplet dynamics (Maxey and Riley, 1983). For fuel droplets, the equations can be simplified due to the high density ratio $\rho_d/\rho_g \geqslant 100$ to the following form:

$$\frac{dX_i(t)}{dt} = V_i(t), \tag{1}$$

$$\frac{dV_i(t)}{dt} = \frac{U_i(X(t),t) - V_i(t)}{\tau_d} + f_i, \tag{2}$$

$$\tau_d = \frac{4}{3}\frac{\rho_d}{\rho_g}\frac{D^2}{\overline{c_D(Re_d)Re_d}\,v_g}. \tag{3}$$

The droplet relaxation time τ_d is a measure of the ability of the droplet to follow the velocity fluctuations of the gaseous phase. According to Stein (1973), the drag coefficient c_D can be calculated as a function of the droplet Reynolds number $Re_d = c_{rel}D/v_g$:

* Corresponding author.
E-mail address: goeran.klose@its.uni-karlsruhe.de (G. Klose).

0142-727X/01/$ - see front matter
PII: S0142-727X(01)00097-2

Notation

c_D	drag coefficient
c_{rel}	$\|U - V\|$
CT	crossing trajectories parameter
C_μ, C_T	turbulence model constants
f	body force
D	droplet diameter
k	turbulent kinetic energy
L	length scale
Re	Reynolds number
R	autocorrelation coefficient
St	Stokes number
t	time
T	time scale
U, u	gas velocity
V	droplet velocity
X, x	coordinate
$\overline{Y^2}$	dispersion coefficient

Greeks

ϵ	turbulent dissipation rate
v	kinematic viscosity
ρ	density
τ	time scale

Subscripts

e	eddy
i, j	coordinate directions
g, d	gas, droplet
RMS	Root Mean Square value
t	turbulent
50	volumetric mean
$\perp$	perpendicular to the mean flow

$$c_D = 0.36 + 5.48 Re_d^{-0.573} + \frac{24}{Re_d}. \quad (4)$$

For $Re_d \leqslant 1$, Eq. (4) turns into the Stokes law $c_D = 24/Re_d$, and Eq. (2) becomes a linear differential equation. In order to reflect the effect of the turbulent fluctuations of the gaseous phase on the droplet movement, the instantaneous velocity vectors of the gaseous phase

$$U_i(X(t), t) = \overline{u}_i(X(t)) + u_i'(X(t), t) \quad (5)$$

along the particle trajectories have to be known. As the gaseous velocity fluctuations are not available within common turbulence models, it is the task of a particle turbulence model to provide a procedure for regeneration of the fluctuations $u_i'(X_{(t)}, t)$. The velocity fluctuations essentially depend on global turbulence quantities (e.g., k, ϵ). Additionally, detailed information about the shape of the PDF and the temporal autocorrelation function $R_{ij}(\tau) = \langle u_i'(t), u_j'(t+\tau) \rangle$ of the velocity fluctuations are required. Therefore, empirical assumptions have to be introduced to set up the particle turbulence model. In general, the autocorrelation function reflects the temporal history of the gaseous velocity fluctuations seen by a droplet. All three models studied in the present work are based on the assumption that the PDF of the gas velocity fluctuations has a Gaussian shape with a standard deviation of $u_{RMS} = \sqrt{2k/3}$ being characteristic for isotropic turbulence. The particle turbulence models, to be discussed subsequently, can be distinguished by the shape of their underlying autocorrelation function $R_{ij}(\tau)$. In general, the fluctuations seen by a droplet depend on the local structure of the turbulence as well as on the relative motion between the droplet and the gas. By increasing the relative velocity, the fluctuations along the droplet trajectory become more uncorrelated and therefore the turbulent dispersion of the particle decreases. This is called the "effect of crossing trajectories" (CT effect) (Yudine, 1959).

2.1. The eddy lifetime approach of Gosman and Ioannides

The eddy lifetime approach is based on the assumption that particles mainly respond to low frequency fluctuations of the turbulent eddies. Therefore, the temporal velocity variation seen by a particle can be approximated by a stepwise profile ignoring the high frequencies of the turbulent fluctuations. The effective eddy interaction time intervals τ_g in which the velocities are kept constant are set to the minimum of the integral eddy lifetime T_e and the time scale for the crossing of the eddies τ_{drift} in order to account for the turbulence structure of the gaseous phase as well as for the CT effect (Fig. 1).

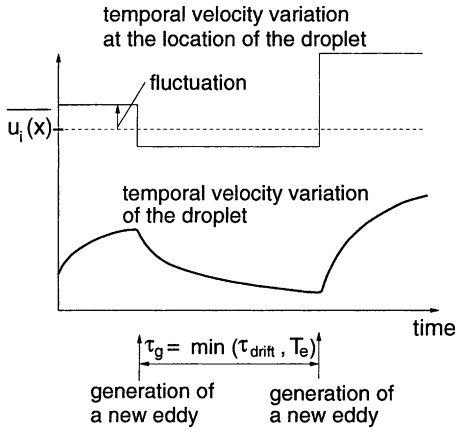

Fig. 1. Estimation of effective eddy interaction time.

$$T_e = \frac{L_e}{|u_g'|} = \frac{C_\mu^{1/2} k^{3/2}}{\epsilon |u_g'|}, \quad (6)$$

$$\tau_{drift} = -\tau_d \ln\left(1 - \frac{L_e}{\tau_d c_{rel}}\right). \quad (7)$$

According to Gosman and Ionnides (GI model), the relevant time scales can be estimated by Eqs. (6) and (7). Eq. (7) is based on a solution of Eqs. (1) and (2) and on the assumption of Stokes flow and a constant local gas velocity. The model constant C_μ has a value of 0.09.

2.2. The eddy lifetime approach of Milojević

The model of Milojević (M model) is similar to the previous one. An eddy lifetime approach is used to capture the impact of the turbulence on the particle propagation by interaction with eddies of integral scale. In contrast to the previous model, the CT effect is accounted for by simultaneously tracking the trajectories of the particle and a fluid point which characterizes the center of the current eddy (Fig. 2) influencing the particle.

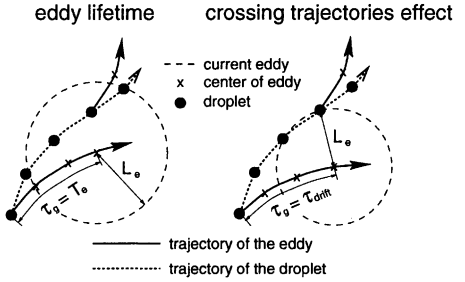

Fig. 2. Estimation of effective eddy interaction time.

$$T_e = C_T \frac{k}{\epsilon}, \tag{8}$$

$$L_e = T_e u_{RMS} = \sqrt{\frac{2}{3}} C_T \frac{k^{3/2}}{\epsilon}. \tag{9}$$

A new instantaneous velocity of the gaseous phase will be generated either when the current eddy reaches its lifetime or when the distance between the fluid point and particle exceeds the integral length scale L_e of the eddy. The integral time and length scales of the eddies are calculated according to Eqs. (8) and (9). The constant C_T was chosen as 0.3.

2.3. The spectral dispersion model of Blümcke

Contrary to the eddy lifetime models, in the spectral dispersion model of Blümcke (B model) velocity fluctuations are generated from an explicitly specified autocorrelation function. However, due to the slip between the particles and the gaseous phase, the autocorrelation function of the gas velocities along the particle trajectory cannot be estimated in advance. Therefore, this model is based on Lagrangian as well as Eulerian autocorrelation functions which can be specified explicitly. Similar to the previous model, trajectories of the particle and a fluid point are tracked simultaneously. The velocity fluctuations along the trajectory of the fluid point are generated with respect to the given Lagrangian autocorrelation function $R(\tau)$. Based on the instantaneous velocity of the fluid point, the velocity fluctuations at the particle are determined as function of the distance between the fluid point and the particle from a given spatial Eulerian correlation function $R(\Delta x)$ (Fig. 3).

$$R_{(\tau)} = e^{-\tau/T_e}, \tag{10}$$

$$R_{(\Delta x)} = e^{-\Delta x/L_e}. \tag{11}$$

An exponential function was chosen by Blümcke for representing the temporal and spatial decay of the autocorrelation coefficients (Eqs. (10) and (11)). The integral scales T_e, L_e are determined from Eqs. (8) and (9). The algorithm for generating the correlated fluctuations is based on a digital filter by which a sequence of uncorrelated velocity fluctuations produced by a random generator is correlated. A detailed description of the filter function is given by Blümcke (1992) and Rembold (1999). For capturing the whole range of the turbulent energy spectrum, the temporal and spatial steps between two succeeding fluctuations are about three orders of magnitude smaller than the associated integral scales.

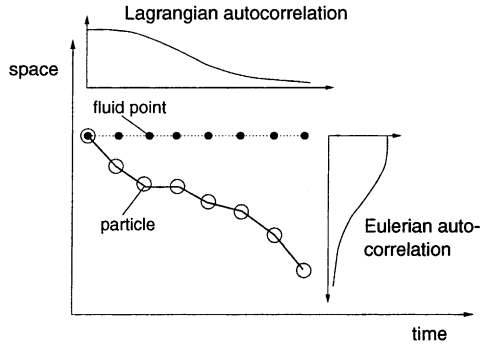

Fig. 3. Temporal and spatial correlations of the Blümcke model.

3. Prediction of single particle dispersion

Due to its exactly specified boundary conditions, the experiment by Snyder and Lumley (1971) has been used in this study for validation of the droplet turbulence models. The test rig used by Snyder and Lumley was a vertically arranged channel with a quasi-homogeneous air flow characterized by decaying turbulence. Single particles were injected into this flow and photographically tracked. By observing a large number of particles, information about the standard deviation $\overline{Y^2} = \langle (X_\perp - \overline{X_\perp})^2 \rangle$ of the particle number density distribution, the kinetic energy and the velocity autocorrelation function of the particles were obtained. Particles of different density and diameter have been investigated by Snyder and Lumley.

Due to the interaction of the inert particles with the gravitational force aligned with the axis of the channel, the different particle types are characterized by a specific drift velocity. Therefore, the turbulent dispersion of the particles was affected by the CT effect. Four particle types, shown in Table 1, which are characterized by different particle relaxation times τ_d were investigated.

In Fig. 7 the predictions of the three models are compared to the experimental results of Snyder and Lumley. The comparison includes the temporal evolution of the standard deviation $\overline{Y^2}$ and of the autocorrelation function $R(\tau)$ of the particles.

The GI model is found to underpredict the dispersion of the light particles (hollow glass) and to overpredict the dispersion of the heavy particles (glass, copper). However, the prediction of the dispersion of the corn pollen agrees well with the measurements. The discrepancy with the experimental data has two main causes. According to the GI model, the eddy lifetime T_e is estimated by dividing the turbulent integral length scale by the magnitude of the current gas phase velocity fluctuation. This procedure is justified when the vectors of the particle velocity and the mean gas velocity are approximately equal ($V \approx \overline{U}$). This condition can only be satisfied by particles of medium inertia being too heavy to adjust to the turbulent gas fluctuations but light enough to adapt quickly to the mean gas velocity. However, when the particle relaxation time τ_d becomes larger, the assumption of Stokes flow is no longer valid due to the increasing drift velocity. Therefore, the crossing time scale τ_{drift} is overpredicted by the GI model (Eq. (7)) causing an overprediction of the dispersion.

When using the M model as well as by the B model the integral time scale T_e is derived from a correlation and more sophisticated methods are applied to account for the CT effect. Therefore, these models are capable of better predicting the

Table 1
Particle types investigated by Snyder and Lumley

	Hollow glass	Glass	Pollen	Copper
τ_d (ms)	1.7	45.0	20.0	49.0

turbulent particle dispersion. The M model is based on generating eddies of an integral scale lasting for time intervals given by Eq. (8). Due to the quasi-homogeneous character of the gaseous phase, the M model reveals overshoots in the prediction of the hollow glass beads that are not affected by the CT effect. The results of the B model coincide well with the experimental data for all particle types.

The calculated autocorrelation functions of all models exhibit a slower decay compared to the gaseous phase. This result is in contradiction to the experimental data showing a faster decrease of the autocorrelation functions of the particles. These differences are probably caused by the empirical character of the correlations used for the estimation of T_e.

4. Dispersion of a polydisperse spray

As a practical test case, a fuel spray that has been previously investigated experimentally at the Institute for Thermal Turbomachinery (Willmann, 1999) was studied. The conditions given in Table 2 reflect the conditions in a premix duct of a Lean-Premix-Prevaporize (LPP) combustor. The geometry of the test section is illustrated in Fig. 4. It consists of an airblast atomizer aligned with the axis of the cylindrical test channel. The atomizer is surrounded by a co-annular air stream shielding the walls from droplet impact. 2-Propanol fuel was used. At the planes $z = 12$ and $z = 210$ mm, detailed measurements of the gaseous phase and the spray were conducted with LDA and PDPA techniques, respectively.

The dispersion of the spray was predicted by the three droplet turbulence models. Additionally, a deterministic spray simulation was carried out to isolate the effects of droplet starting conditions from the turbulent dispersion. The droplet vaporization was accounted for by a Uniform-Temperature model (Schmehl et al., 1998). The area immediately downstream of the atomizer is characterized by secondary droplet breakup. Therefore, the secondary atomization model (Schmehl et al., 1998) developed at the Institute for Thermal Turbomachinery was used. The initial boundary conditions for the spray simulations were obtained by optimizing the droplet starting conditions with respect to the measurements available for plane $z = 12$ mm. In Fig. 4 the discretization of the angular and diameter dependent distribution of the liquid volume flux is shown. The distribution of the droplet velocity magnitude at the atomizer edge was assumed to be of Gaussian shape ($\bar{V} = 15$ m/s, $V_{RMS} = 2.5$ m/s).

Table 2
Operating conditions

Mass flow gas $\dot{m}_{gas}$	517 g/s
Pressure	8 bar
Gas temperature	500 K
Mass flow liquid	0.122 g/s

Due to the weak fuel loading the gaseous phase is not significantly affected by the spray. Therefore, the flow field was calculated prior to the spray simulations and found to be in good agreement with the experiment. The flow field just behind the atomizer is characterized by two coaxial recirculation zones in the wake of the atomizer. Further downstream ($z \geqslant 20$ mm), the flow field is typical for two coaxial mixing jets.

A comparison between the experimental data and the prediction of the liquid volume flux is shown in Fig. 5. The good agreement between the predicted and measured volume flux distribution in plane $z = 12$ mm confirms the assumptions made for the droplet initial parameters. The coincidence of the results of the laminar and turbulent calculations emphasizes that the dispersion process has no significant effect on the flux distribution in this plane. In plane $z = 210$ mm, however, a comparison between the deterministic and turbulent simulations reveals a significant influence of the turbulent dispersion on the spray propagation. In contradiction to the experiment of Snyder and Lumley no major differences between the different models can be distinguished which can probably be attributed to the polydisperse character of the spray smoothing out the dispersion characteristics of the different droplet classes. The shortcomings of the GI model revealed for heavy and light particles (see Section 3) obviously are compensating for each other.

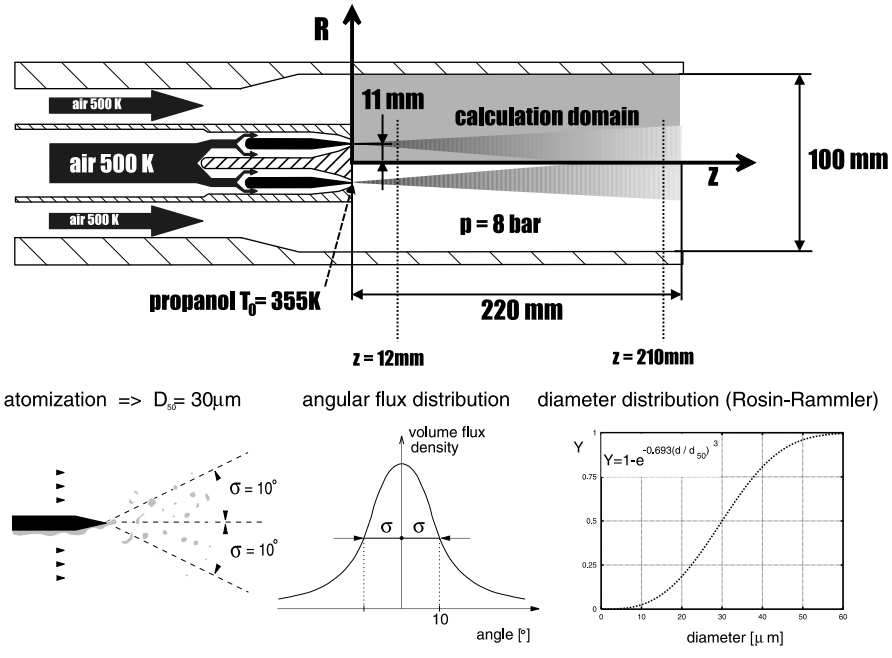

Fig. 4. Geometry of the LPP test rig.

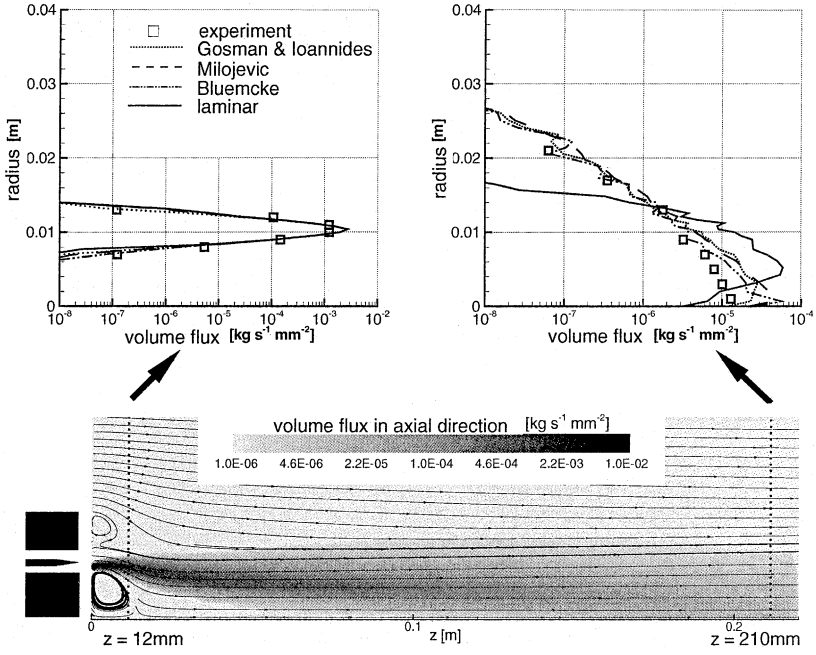

Fig. 5. Axial liquid volume flux.

5. Parametric study of the dispersion under combustor conditions

Typical combustor sprays are characterized by a wide range of droplet diameters and relative velocities between the droplets and the gaseous phase. Thus, the turbulent dispersion varies substantially. The turbulent dispersion can be characterized by the Stokes number $St = \overline{\tau_d}/T_e$ reflecting the influence of the particle inertia and the crossing trajectory parameter $CT = \overline{c_{rel}}/u_{RMS}$ which accounts for the CT effect.

Subsequently, a parametric study covering a wide range of possible combustor operational conditions is presented exceeding the range of the experiment of Snyder and Lumley. The analysis is based on the B model. The ranges covered are

$$0 \leqslant St \leqslant 40, \tag{12}$$

$$0 \leqslant CT \leqslant 50. \tag{13}$$

When deviating from Stokes flow, Eq. (2) becomes nonlinear resulting in a non-Gaussian shape of the PDF of the drag forces acting on the droplet. Therefore, the parameters listed above are not sufficient to characterize the statistics of the dispersion process. However, the deviation from Stokes flow scales with the droplet Reynolds number (cf. Eq. (4)). On the

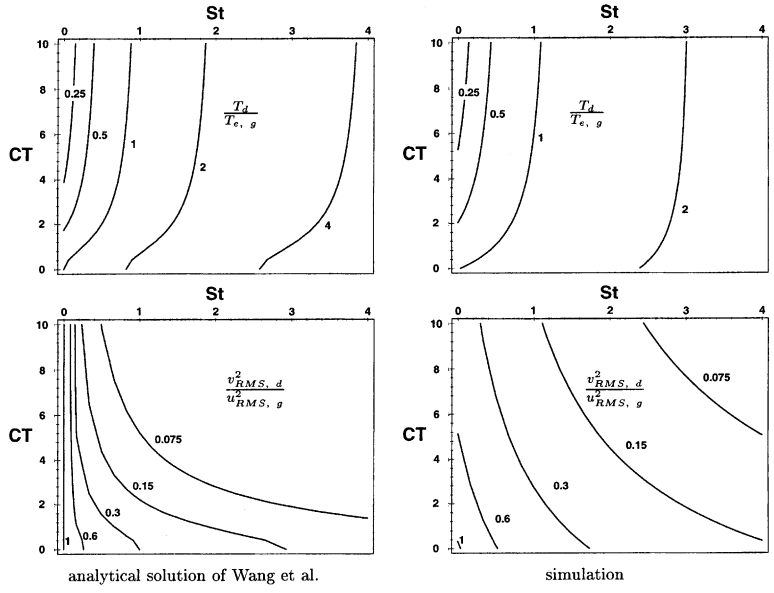

Fig. 6. Dependency of the integral time scale and energy on St and CT.

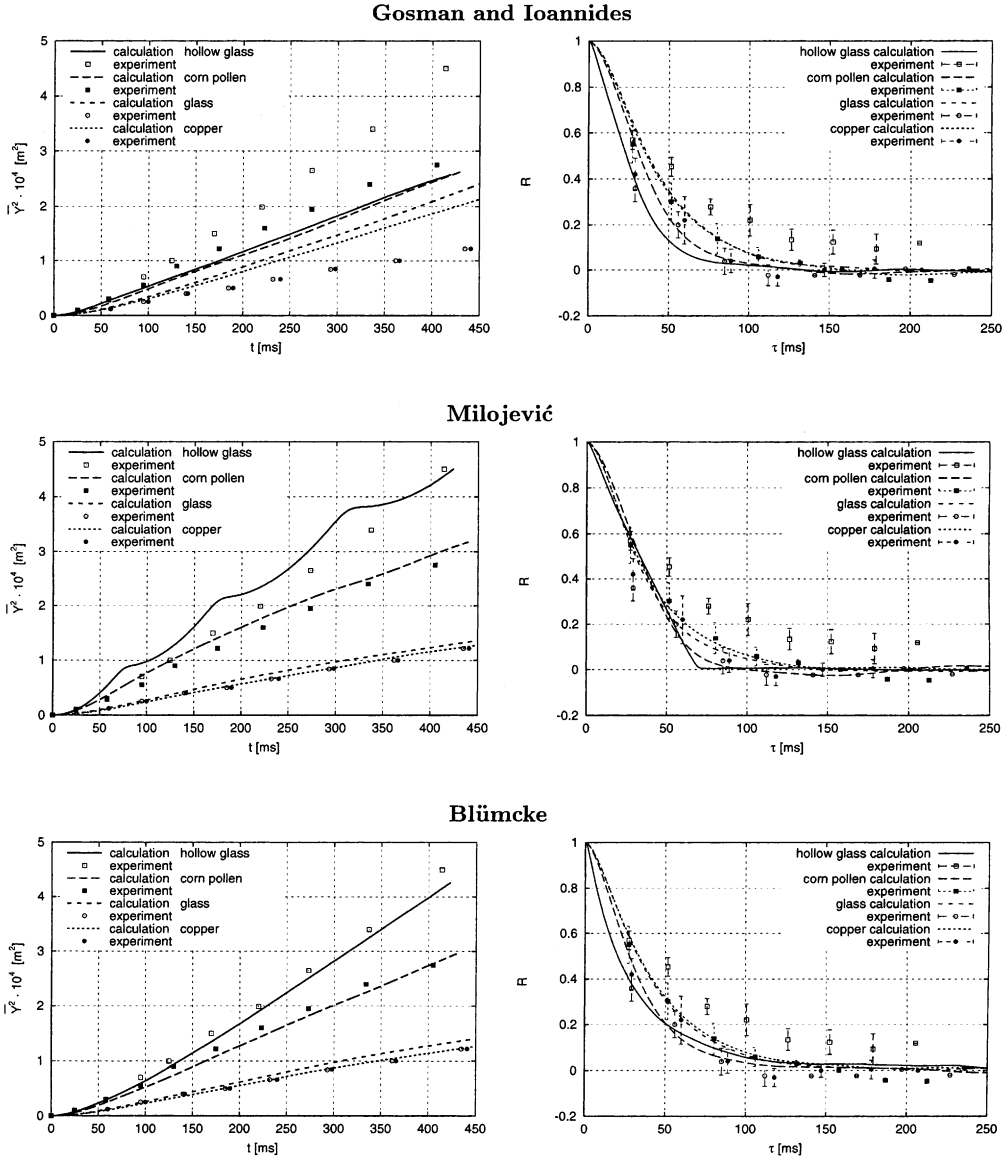

Fig. 7. Dispersion and autocorrelation functions of the experiment of Snyder and Lumley.

basis of a dimensional analysis and by assuming that the fluctuations of c_{rel} are characterized by u_{RMS} $\left(\left(\overline{c_{\mathrm{rel}}^2}\right)^{1/2} \approx u_{\mathrm{RMS}}\right)$, a turbulent droplet Reynolds number

$$Re_{\mathrm{d,t}} = \frac{u_{\mathrm{RMS}} D}{\nu_{\mathrm{g}}} \tag{14}$$

can be introduced. By keeping St, CT and $Re_{\mathrm{d,t}}$ constant, the shape of the PDF of the drag forces is fixed allowing a characterization of the dispersion statistics. For combustor flows, a value of $Re_{\mathrm{d,t}} = 5$ was found to be representative and was used in this study.

The resulting distributions of the turbulent kinetic energy $v^2_{\mathrm{RMS,d}}$ of the droplets and their integral turbulent time scale T_{d} as a function of St and CT are plotted in Fig. 6. For large values of St and CT, the droplet kinetic energy approaches very rapidly to zero resulting in almost no dispersion. Therefore, only the range $0 \leqslant St \leqslant 4$, $0 \leqslant CT \leqslant 10$ where a significant dispersion is found is presented. The numerical results are compared to an analytical solution derived by Wang and Stock (1993). Fig. 6 reveals that the droplet dispersion strongly depends on the St number whereas the CT number has a weaker influence. The analytical solution of Wang and Stock is in good qualitative agreement with the simulations. The integral time scale of the droplet fluctuations is even in a good quantitative agreement for $St < 1$. However, the quantitative differences between both approaches increase with increasing St and CT numbers. These differences are attributed to the fact that the analytical solution of Wang and Stock was derived on basis of the Stokes flow and does not account for the effect of the nonlinear drag fluctuations at $Re_{\mathrm{d,t}} > 1$. Finally, correlations of the turbulent kinetic energy of the droplets and their integral time scale were fitted to the results of this fundamental study giving the subsequent relations.

Turbulent kinetic energy:

$$\frac{\overline{u^2}}{u^2_{\mathrm{RMS,g}}} = a + F(Sto, b, c, d) + F(CT, e, f, g) + F(Sto, h, c, d)F(CT, 1, f, g), \tag{15}$$

$a = -0.04280308209808592,$
$b = 0.508539661884366592,$
$c = -0.537834404167855616,$
$d = -0.415967038205374912,$
$e = 0.26728522574548416,$
$f = -4.70481422899973056,$
$g = -3.93429107821800064,$
$h = 19.8525654634876576.$

Integral time scale:

$$\frac{T_{L,P}}{T_L} = a + F(Sto, b, c, d) + F(CT, e, f, g) + F(Sto, h, c, d)F(CT, 1, f, g), \quad (16)$$

$a = 6.3139978073363008,$
$b = -4.65656195908919488,$
$c = -0.890569367811421312,$
$d = 3.07708119458826048,$
$e = -12.3905710730065136,$
$f = -1.44245297144525344,$
$g = 1.80229809887799808,$
$h = 14.872722752227984.$

The function F is defined as

$$F(X, p, q, r) := p\left\{\frac{1}{2} + \frac{a\tan((X-q)/r)}{\pi}\right\}. \quad (17)$$

6. Conclusions

In this paper, different models for predicting droplet dispersion in turbulent flows were assessed.

As a first generic test case, the dispersion of particles in a quasi-homogeneous isotropic turbulent flow was studied. It was found that the accuracy of the eddy lifetime approach proposed by Gosman and Ioannides is limited to a narrow range of Stokes numbers $St \approx 2$ and to small relative velocities between the gaseous phase and the droplet. However, the eddy lifetime model of Milojević as well as the spectral dispersion model of Blümcke performed well over the total range of Stokes numbers and relative velocities (see Fig. 7).

It was also shown that the differences between the three models seem to play a minor role in the overall prediction of jet engine combustors due to compensating effects. However, for very small or very large fuel droplets the results of the dispersion model of Gosman and Ioannides have to be inspected carefully in terms of accuracy.

As a general objective, this study was extended to a wide range of dispersion conditions typical for combustors. A turbulent droplet Reynolds number was introduced to extend the characterization of droplet dispersion to non-Stokesian regimes. For the interesting range of $0 < St < 4$ it was found that the Stokes number is the parameter which mostly effects droplet dispersion. The crossing trajectories parameter CT characterizing the effect of the slippage between droplets and the gas was found to have a much weaker effect.

References

Berlemont, A., Desjonquéres, P., Gouesbet, G., 1990. Particle Lagrangian simulation in turbulent flows. Int. J. Multiphase Flow 16 (1), 19–34.

Blümcke, E., 1992. Turbulente Partikeldispersion in eingeschlossenen Drallströmungen. Ph.D. thesis, Deutsche Forschungsanstalt für Luft- und Raumfahrt, Ruhr-Universität Bochum, Köln.

Chen, X.O., Pereira, J.C.F., 1994. Comparison of the various particle dispersion models in plane mixing shear layers. Numerical Methods in Multihase Flows, American Society of Mechanical Engineering FED-Vol. 185, pp. 217–225.

Dutta, P., Sivathanu, Y.R., Gore, J.P., 1997. Discrete probability function method for the calculation of turbulent particle dispersion (TN). AIAA J. 35 (1), 200–202.

Gosman, A.D., Ioannides, E., 1983. Aspects of computer simulation of liquid–fueled combustors. J. Energy 7 (6), 482–490.

Klose, G., Rembold, B., Koch, R., Wittig, S., 2000. Comparison of state of the art droplet–turbulence interaction models for aeroengine combustor conditions. In: Nagano, T.T.Y., Hanjalić, K. (Eds.), Proceedings of the Third International Symposium on Turbulence, Heat and Mass Transfer, Nagoya, vol. 3, pp. 763–770.

Maxey, M.R., Riley, J.J., 1983. The equation of motion for small rigid particle sphere in a nonuniform flow. Phys. Fluids 26, 883–889.

Milojević, D., 1990. Lagrangian Stochastic-Deterministic (LSD) prediction of particle dispersion in turbulence. Part. Part. Syst. Charact. 7, 181–190.

Rembold, B., 1999. Untersuchung mathematischer Modelle zur Beschreibung der Ausbreitung von Sprühstrahlen in turbulenten Strömungen. Master's thesis, Institut für Thermische Strömungsmaschinen, Universität Karlsruhe (TH).

Schmehl, R., Klose, G., Koch, R., Wittig, S., 1998. Droplet Evaporation and Transport, Tech. Report, BRITE/EURAM Low NO_x Phase III. Institut für Thermische Strömungsmaschinen, Universität Karlsruhe, TH.

Schmehl, R., Klose, G., Maier, G., Wittig, S., 1998. Efficient numerical calculation of evaporating sprays in combustion chamber flows. In: Proceedings of the 92nd Symposium on Gas Turbine Combustion, Emissions and Alternative Fuels, RTO Meeting Proceedings, vol. 14, Lisbon, 1998.

Snyder, W.H., Lumley, J.L., 1971. Some measurements of particle velocity autocorrelation functions in a turbulent flow. J. Fluid Mech. 48, 41–71.

Stein, W.A., 1973. Berechnung der Verdampfung von Flüssigkeit aus feuchten Produkten im Sprühturm. Verfahrenstechnik 7 (9), 262–267.

Wang, L.P., Stock, D.E., 1993. Dispersion of heavy particles by turbulent motion. J. Atmos. Sci. 50 (13), 1897–1913.

Willmann, M., 1999. Charakterisierung eines Airblastzerstäubers-Bestätigung numerischer Simulationen mit einem angepaßten Phasen-Doppler-Tropfenmeßverfahren. Ph.D. thesis, Institut für Thermische Strömungsmaschinen, Universität Karlsruhe (TH).

Yudine, M.L., 1959. Physical considerations on heavy-particle diffusion. Adv. Geophys. 6, 185–191.